Physics Letters A 424 (2022) 127847

Contents lists available at ScienceDirect

Physics Letters A

www.elsevier.com/locate/pla

Chimera states in a multi-weighted neuronal network

Iqtadar Hussain [a,*], Sajad Jafari [b,c], Matjaž Perc [d,e,f], Dibakar Ghosh [g]

[a] Mathematics Program, Department of Mathematics, Statistics and Physics, College of Arts and Sciences, Qatar University, 2713, Doha, Qatar
[b] Health Technology Research Institute, Amirkabir University of Technology (Tehran polytechnic), Iran
[c] Department of Biomedical Engineering, Amirkabir University of Technology (Tehran polytechnic), Iran
[d] Faculty of Natural Sciences and Mathematics, University of Maribor, Koroška cesta 160, 2000 Maribor, Slovenia
[e] Department of Medical Research, China Medical University Hospital, China Medical University, Taichung, Taiwan
[f] Complexity Science Hub Vienna, Josefstädterstraße 39, 1080 Vienna, Austria
[g] Physics and Applied Mathematics Unit, Indian Statistical Institute, 203 B. T. Road, Kolkata 700108, India

ARTICLE INFO

Article history:
Received 6 October 2021
Received in revised form 6 November 2021
Accepted 17 November 2021
Available online 22 November 2021
Communicated by B. Malomed

Keywords:
Synchronization
Chimera
Neuronal network
Multi-weighted network
Directed links

ABSTRACT

There are multiple types of interactions among neurons, each of which has a remarkable effect on the neurons' behavior. Due to the significance of chimeras in neural processes, in this paper, we study the impact of different electrical, chemical, and ephaptic couplings on the emergence of chimera. Consequently, a multi-weighted small-world network of neurons is considered. The simultaneous effects of two and three couplings are explored on the chimera and complete synchronization. The results represent that the synchronization is achieved in very small coupling strengths in the absence of chemical synapses. In contrast, without electrical synapses, the neurons only exhibit chimera behavior. In the three-weighted network, the synchronization is enhanced for special chemical coupling strengths. The network with directed links is also examined. The general behaviors of the directed and undirected networks are the same; however, the directed links lead to lower synchronization error.

1. Introduction

Synchronization is one of the essential collective behaviors in complex dynamic networks [1]. Numerous studies have been done on this phenomenon in coupled systems in various fields of science and engineering, including biology [2]. These studies have shown that the synchronized behavior of the systems depends on many factors, including the topology of the network and the coupling configuration [3,4]. In the nervous system, several neural processes are accompanied by synchronous firings. Some of its valuable applications are cognitive tasks, learning, and memory [5,6]. In contrast, synchronization may emerge in some pathological diseases such as Parkinson's disease, Alzheimer's disease, etc. [7,8]. Consequently, a bunch of researches have been concentrated on the synchronous behavior of the coupled neurons [9–13].

One of the exceptional cases of synchrony in coupled oscillators is the simultaneous existence of synchronization and asynchronization in the network [14]. This particular situation, termed chimera state, has been reported in massive studies of physical, chemical, and biological oscillators [15]. Extensive investigations of chimeras have been done in coupled neural models with the motivation of the advent of chimera-like behavior in neuronal functions, including uni-hemispheric sleep, neural bumps, etc. [16–21]. The occurrence of chimera has been found in a variety of coupled neuron models in complex networks [22], multilayer structures [23], time-variant topologies [24], hierarchical and fractal connectivity [25]. Simo et al. [26] reported the appearance of the chimera state, multi-chimera, alternating chimera, and multi-cluster traveling chimera in the coupled Hindmarsh-Rose neurons with considering the electric field. Rontogiannis et al. [27] investigated the impact of the reflecting connectivity as a model of the brain hemispheres' connections on the coupled FitzHugh-Nagumo oscillators. Ruzzene [28] studied the formation of the chimera states in a multilayer neuronal network and presented a controller by using the pacemaker oscillator to adjust the positions of the synchronous and asynchronous groups.

The communications among neurons occur through different ways of information transmissions. The first type of transmission is the chemical synapse accompanied by the release of neurotransmitters from the pre-synaptic neurons [29,30]. The post-synaptic neuron then receives the transmitter. The second type is through the electrical synapses, in which the transmissions occur directly via the channels (gap junctions) between neurons [31,32]. It has

* Corresponding author.
E-mail address: iqtadarqau@gmail.com (I. Hussain).

https://doi.org/10.1016/j.physleta.2021.127847
0375-9601/

been revealed that the neurons' communication results from both of these transmissions rather than one of them [33–35]. Besides the synaptic transmissions, the membrane potential of the neurons is influenced by the ephaptic coupling [36,37]. The ephaptic coupling refers to the effects of the electric fields outside the neurons' membranes. To consider the ephaptic impact, scientists have modified the neuronal models by adding the magnetic flux with using memristors [38–40]. The effect of ephaptic coupling on the synchronization and chimera has been investigated in several studies [41–45].

This paper aims to investigate the simultaneous effects of different interactions on the emergence of synchronization and chimera. In the previous studies, the chimera and synchronization have been explored with considering hybrid electrical and chemical connections [46,23,47–50]. In these studies, the type of connections for the synapses is considered differently. For example, a multilayer network has been constructed, and the chemical and electrical synapses have been used as the interlayer and intralayer links [23]. In other studies, these synapses were applied as the different links of a modular structure [49], or a hyper network [47]. Here, we assume the same structure for the synapses (small-world), and also, the links are weighted. Furthermore, we include the ephaptic coupling, which had not been considered with other couplings so far. Therefore, a multi-weighted network is constructed with three weighted small-world structures to model the electrical, chemical, and ephaptic couplings. The network is solved in different cases, and the synchronization error and the strength of incoherence are calculated numerically. It is observed that the electrical synapses have an important role in enhancing the synchronization among neurons, without which the synchrony is not achieved and neurons develop in the chimera state. Furthermore, in the presence of all couplings, the synchronization is enhanced in special chemical coupling strengths. Then, the links are considered to be directed, and investigations are repeated. The results represent that the directed links cause the lower synchronization error. The regions of different dynamical behaviors are obtained in each case.

2. The neuronal network with multi-weights

A complex multi-weighted network with N nodes and k weights between the nodes can be described by,

$$\begin{aligned}\dot{X}_i &= f(X_i) + \epsilon_1 \sum_{j=1}^{N} a_{ij}^1 w_{ij}^1 H_1(X_j) + \epsilon_2 \sum_{j=1}^{N} a_{ij}^2 w_{ij}^2 \\ & H_2(X_j) + \cdots + \epsilon_k \sum_{j=1}^{N} a_{ij}^k w_{ij}^k H_k(X_j),\ i = 1, 2, \cdots, N\end{aligned} \tag{1}$$

where X is the d-dimensional state vector, $f(X)$ is the evolution function of the single node, $\epsilon_1, \epsilon_1, ..., \epsilon_k$ are the coupling strengths of each weighted subnetwork, and $H_1(X), ..., H_k(X)$ are the inner coupling functions. The topology of the subnetworks is defined by the matrices $A^k = [a_{ij}^k]_{N\times N}$, with $a_{ij}^k = 1$ if the ith and jth nodes are connected, and $a_{ij}^k = 0$, else. The matrices $W^k = [w_{ij}^k]_{N\times N}$ define the weights of the links of the subnetworks.

Here, the Fitzhugh-Nagumo model with electromagnetic induction [51] ($X = [u, v, \phi]$) is used to describe the dynamics of each node of the network ($f(X) = f(u, v, \phi)$) as,

$$\begin{aligned}\dot{u} &= u(u-a)(1-u) - v + k_3 u\rho(\phi), \\ \dot{v} &= \varepsilon(u - dv), \\ \dot{\phi} &= k_1 u - k_2\phi + \phi_{ext},\end{aligned} \tag{2}$$

where u, v and ϕ show the membrane potential, the slow current variable, and the magnetic flux. The parameter a plays an important role in the fast dynamics and is usually set at $a > 0$ to preserve the electrophysiological meaning [52]. Here, the parameters are kept at $a = 0.5, \varepsilon = 0.02, d = 1$ in which the non-memristive model represents the resting state. $\rho(\phi)$ is the flux-controlled memristor, considered as $\rho(\phi) = \alpha + 3\beta\phi^2$ with $\alpha = 0.1$ and $\beta = 0.02$, and the parameters of the memristor are adjusted as $k_3 = 1, k_1 = 0.5, k_2 = 0.9, \phi_{ext} = 2.4$ in which the neuron spikes regularly [51]. The topology of all subnetworks is considered to be small-world with probability $p = 0.1$, and each node is connected to its four nearest neighbors, i.e., two nodes from each side. The weights of all links are determined randomly in $(0, 1]$. Here, we consider three subnetworks ($k = 3$) regarding the interactions among neurons which can be through electrical synapses (H_1), chemical synapses (H_2), and ephaptic coupling (electromagnetic induction) (H_3). Therefore, we have

$$\begin{aligned}H_1(X_j) &= \begin{bmatrix} u_j - u_i \\ 0 \\ 0 \end{bmatrix},\ H_2(X_j) = \begin{bmatrix} \frac{v_s - u_i}{1+\exp(-\lambda(u_j - \theta_s))} \\ 0 \\ 0 \end{bmatrix}, \\ H_3(X_j) &= \begin{bmatrix} 0 \\ 0 \\ \phi_j - \phi_i \end{bmatrix}\end{aligned} \tag{3}$$

where $v_s = 2, \theta_s = -0.25, \lambda = 10$. The schematic of the multi-weighted network is shown in Fig. 1.

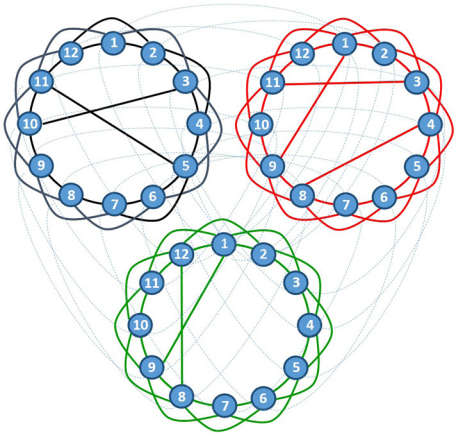

Fig. 1. The schematic of the considered multi-weighted network with 12 nodes. Three subnetworks are illustrated with different colors (red, green, and black) relating to the couplings to represent the multiple weights better. All topologies are considered to be small-world. (For interpretation of the colors in the figure(s), the reader is referred to the web version of this article.)

3. Results

The multi-weighted network with $N = 100$ is solved numerically using the 4th order Runge-Kutta algorithm for 3000 time units with time step 0.01. All of the initial conditions are selected randomly. The network is investigated for different values of coupling strengths $(\epsilon_1, \epsilon_2, \epsilon_3)$. To evaluate the synchronized behavior of the network, the synchronization error is calculated as,

$$E = \left\langle \frac{1}{N-1} \sum_{j=2}^{N} \sqrt{(u_1 - u_j)^2 + (v_1 - v_j)^2 + (\phi_1 - \phi_j)^2} \right\rangle_t. \tag{4}$$

Furthermore, the strength of incoherence [53] is used to distinguish the chimera pattern from the synchronous and asynchronous states. This measure is found by transforming the u_i variables to $z_i = u_{i+1} - u_i$, and splitting N neurons to $M = N/n$ groups of n neurons. Then, the local standard deviation is calculated as $\delta(m) = < \sqrt{\sum_{j=n(m-1)+1}^{nm} (z_i - < z >)^2} >_t$, $m = 1, ..., M$ where

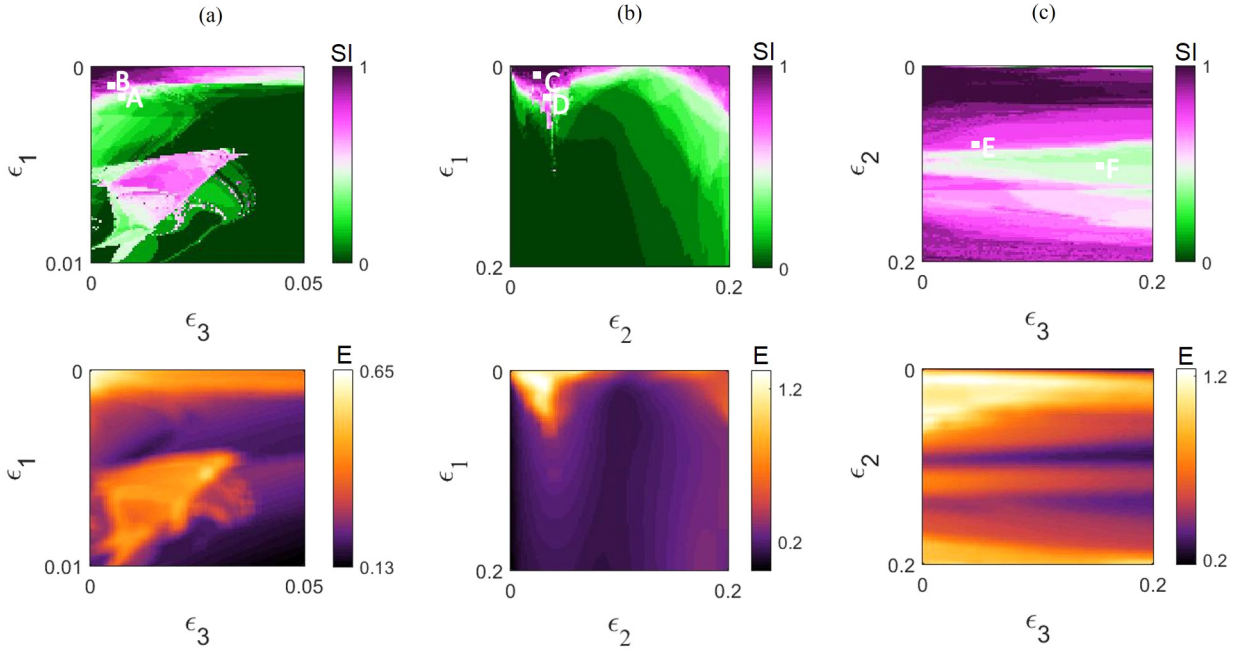

Fig. 2. The strength of incoherence (SI, top row) and the synchronization error (E, bottom row) of the undirected multi-weighted network considering two interactions. (a) In the parameter plane (ϵ_1, ϵ_3), $\epsilon_2 = 0$. (b) In the parameter plane (ϵ_1, ϵ_2), $\epsilon_3 = 0$. (c) In the parameter plane (ϵ_2, ϵ_3), $\epsilon_1 = 0$. When $\epsilon_2 = 0$, the synchronization occurs in weak coupling strengths, while when $\epsilon_3 = 0$, stronger couplings are needed for achieving synchronization. In contrast, in the case of $\epsilon_1 = 0$, the synchronization cannot occur and the pattern is the chimera for any coupling strength values.

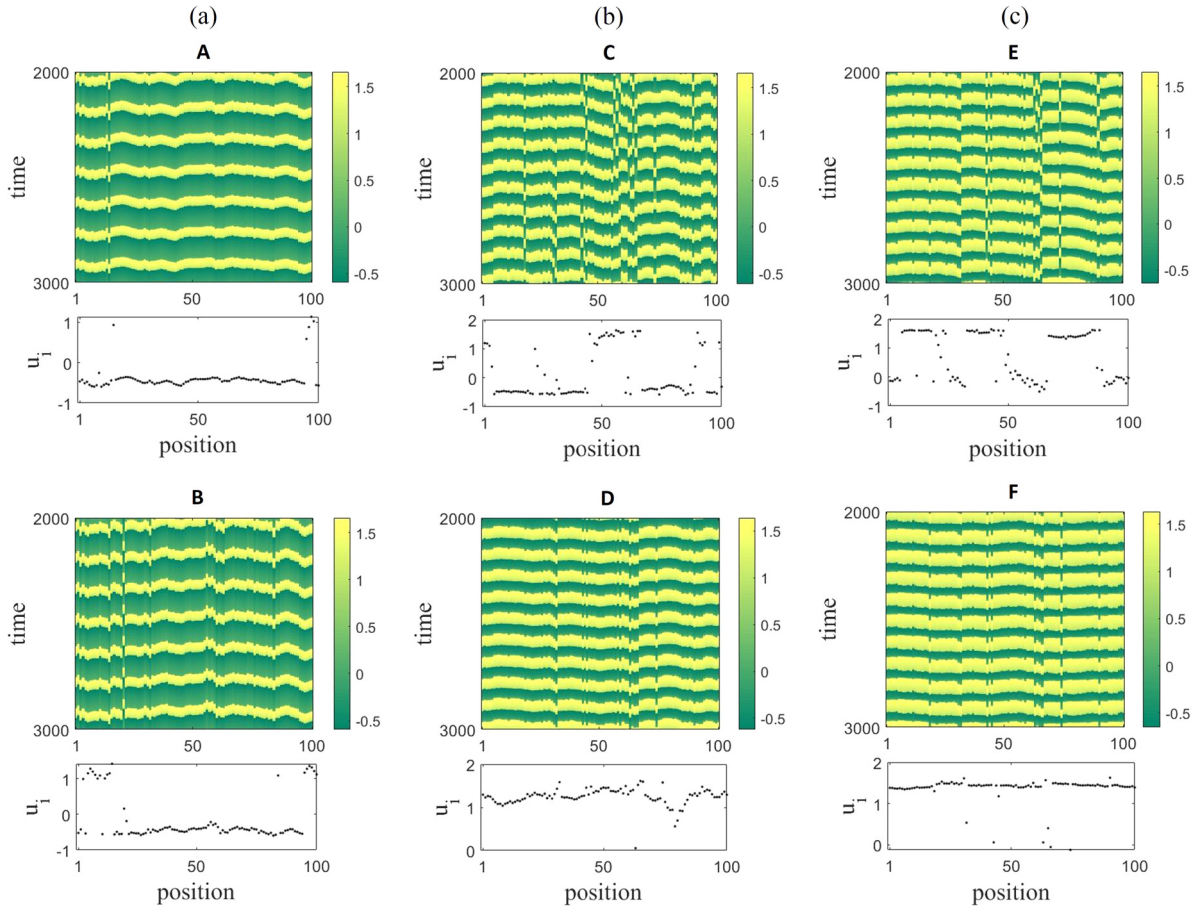

Fig. 3. The evolution of the undirected network with considering two interactions, corresponding to the points specified in Fig. 2. (a) $\epsilon_2 = 0$; A: $\epsilon_1 = 0.0015$, $\epsilon_3 = 0.0065$; B: $\epsilon_1 = 0.0009$, $\epsilon_3 = 0.004$. (b) $\epsilon_3 = 0$; C: $\epsilon_1 = 0.0055$, $\epsilon_2 = 0.0434$; D: $\epsilon_1 = 0.017$, $\epsilon_2 = 0.0532$. (c) $\epsilon_1 = 0$; E: $\epsilon_2 = 0.078$, $\epsilon_3 = 0.05$; F: $\epsilon_2 = 0.01$, $\epsilon_3 = 0.09$. This figure represents different chimera patterns observed with considering two types of couplings.

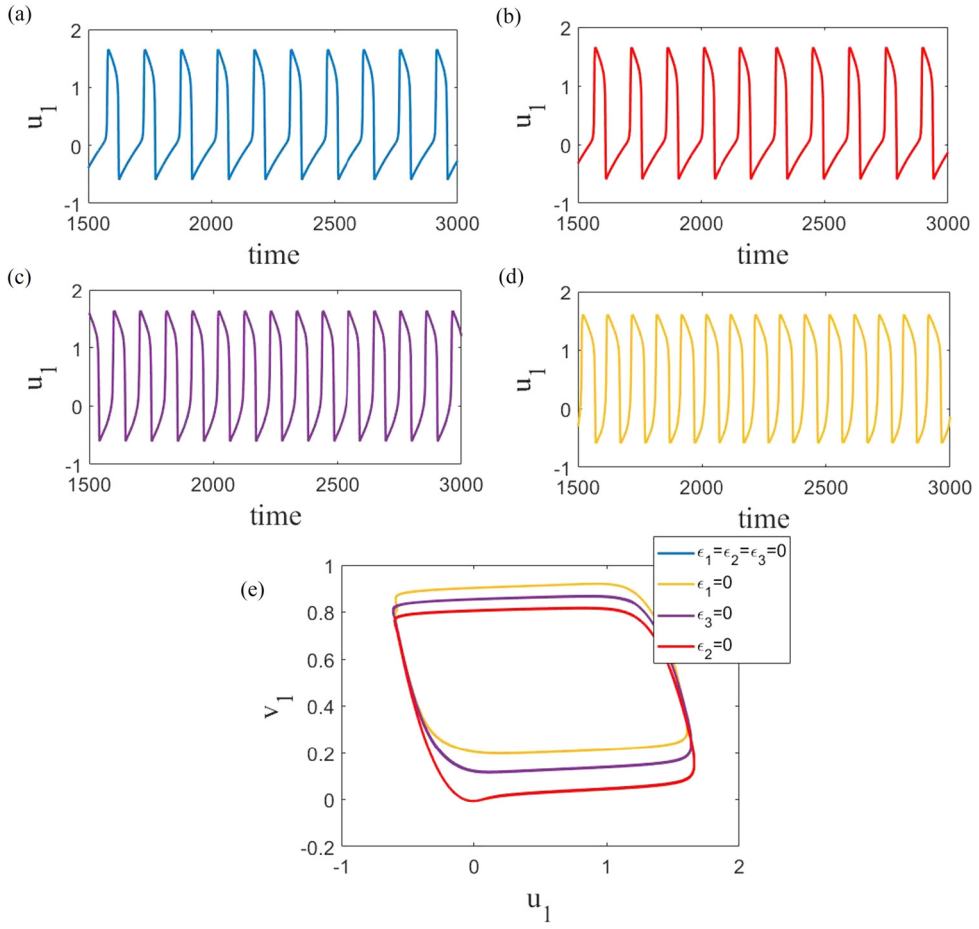

Fig. 4. The time series of the neurons of the network in different coupling configurations: (a) $\epsilon_1 = \epsilon_2 = \epsilon_3 = 0$, (b) $\epsilon_2 = 0$, $\epsilon_1 = 0.0015$, $\epsilon_3 = 0.0065$, (c) $\epsilon_3 = 0$, $\epsilon_1 = 0.0055$, $\epsilon_2 = 0.0434$, (d) $\epsilon_1 = 0$, $\epsilon_2 = 0.078$, $\epsilon_3 = 0.05$, (e) the corresponding attractors. The type of synapses affects the time series and attractor of the neurons.

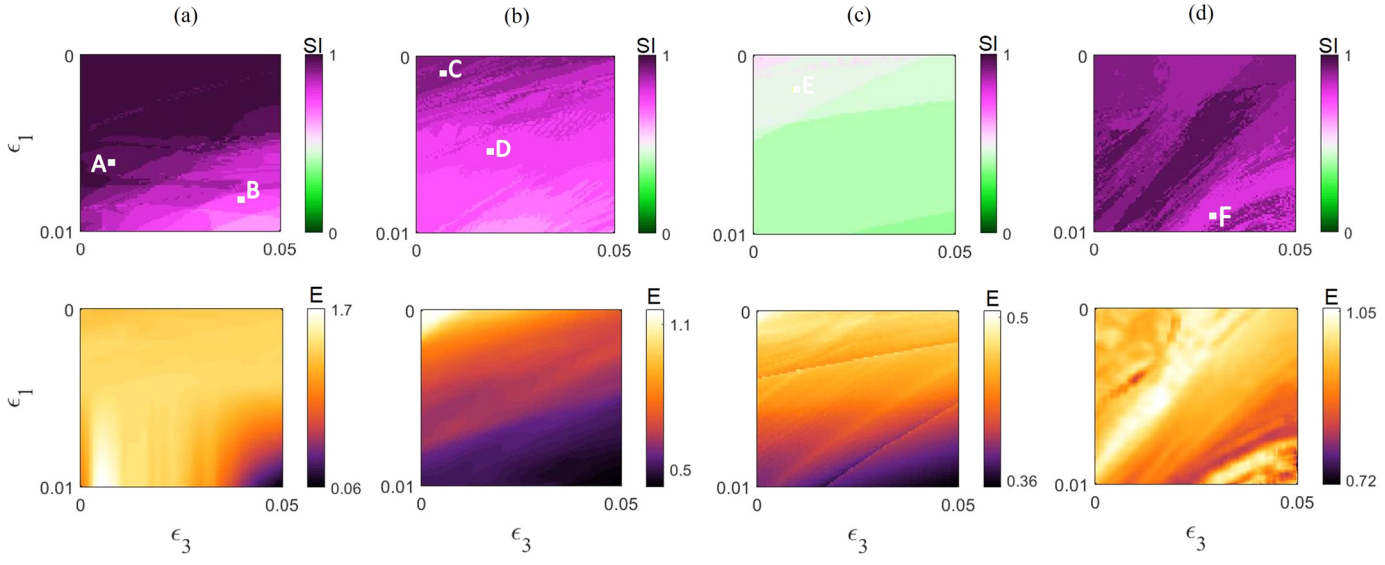

Fig. 5. The strength of incoherence (SI, top row) and the synchronization error (E, bottom row) of the undirected multi-weighted network in the parameter plane (ϵ_1, ϵ_3), for different ϵ_2. (a) $\epsilon_2 = 0.01$, (b) $\epsilon_2 = 0.05$, (c) $\epsilon_2 = 0.1$, (d) $\epsilon_2 = 0.2$. Comparing parts a to d represents that by increasing ϵ_2, the synchronization is enhanced until $\epsilon_2 = 0.1$, and for $\epsilon_2 > 0.1$, it is disturbed.

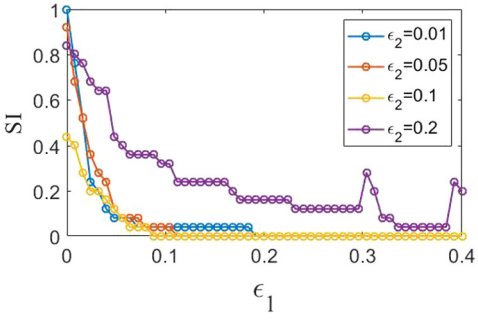

Fig. 6. The strength of incoherence of the undirected multi-weighted network according to ϵ_1, for $\epsilon_3 = 0.05$ and $\epsilon_2 = 0.01, 0.05, 0.1, 0.2$. By increasing the chemical coupling strength, the chimera region shrinks until $\epsilon_2 = 0.1$ and then is enlarged.

$< z >= \frac{1}{N}\sum_{j=1}^{N} z_j$. Thus, the strength of incoherence is obtained with the following equations:

$$s_m = H(t_h - \delta(m)),$$
$$SI = 1 - \frac{\sum_{m=1}^{M} s_m}{M} \tag{5}$$

where $H(\cdot)$ denotes the piecewise Heaviside step function and t_h is a small threshold. Consequently, $SI = 0$, $0 < SI < 1$, and $SI = 1$ defines the synchronous, chimera, and asynchronous states, respectively.

In the first step, the network is considered to be undirected. To realize the simultaneous effect of two types of interactions, firstly, three cases are considered as i) $\epsilon_1 \neq 0, \epsilon_2 = 0, \epsilon_3 \neq 0$, ii) $\epsilon_1 \neq 0, \epsilon_2 \neq 0, \epsilon_3 = 0$, and iii) $\epsilon_1 = 0, \epsilon_2 \neq 0, \epsilon_3 \neq 0$. For each case, two coupling strengths are varied, and synchronization error and strength of incoherence are computed. The results are demonstrated in Fig. 2. By considering the electrical and ephaptic couplings, the network is asynchronous for very small coupling strengths, and the chimera emerges for a slight increase of both coupling strengths. More increases in the coupling strengths result in complete synchronization. Fig. 2a represents a wide synchronization region (dark green region) in this case. However, with increasing coupling strengths, for specific ϵ_1 and ϵ_3, the synchronization is disturbed, and a chimera island is observed. By ignoring the ephaptic coupling and instead considering the chemical interaction, the synchronization decreases among the systems in the weak coupling, and the pattern is mostly the chimera state. As can be seen in Fig. 2b, the complete synchronization appears in stronger electrical coupling strength. Furthermore, higher ϵ_1 is needed for complete synchrony by increasing the chemical coupling strength. Finally, considering the chemical and magnetic couplings does not lead to complete synchronization. Although the level of synchrony changes by varying the chemical and ephaptic interactions, the pattern remains chimera (Fig. 2c).

The behaviors of the network for the points specified in Fig. 2 are represented in Fig. 3. As is shown in part (a) of Fig. 3, there is high synchrony among the neurons when $\epsilon_2 = 0$. Therefore, the pattern is either the chimera state with a large synchronous cluster (B) or the solitary state (A). When $\epsilon_3 = 0$, the pattern and the formed clusters depend highly on the value of the electrical and chemical coupling strengths. Part (b) represents two examples of chimera states in this case. The neurons in the D region are more synchronous than the C region. Finally, two spatiotemporal patterns relating to $\epsilon_1 = 0$ are illustrated in part (c). It should be noted that when $\epsilon_1 = 0$, the most synchronous pattern is the solitary state, and complete synchronization does not occur.

Apart from the collective behavior, the interactions also affect the time series of the systems and their attractors. Fig. 4 depicts the time series and the attractors of the first node of the network relating to the points A, C, and E. The time series of the single node without coupling is shown in Fig. 4a. It can be seen from Fig. 4b that when $\epsilon_2 = 0$, the time series of the systems are similar to the single system. While in the case of $\epsilon_1 = 0$ and $\epsilon_3 = 0$, the time series of coupled systems are different from the single system. The corresponding attractors are demonstrated in Fig. 4e.

Now the multi-weighted network with three types of couplings is considered. Fig. 5 shows the synchronization error and the strength of incoherence in the parameter plane (ϵ_1, ϵ_3) for $\epsilon_2 = 0.01, 0.05, 0.1, 0.2$ in the same region as Fig. 2a. As illustrated in Fig. 2a, there is a wide region of synchronization for $\epsilon_2 = 0$. This region is changed considerably by adding the chemical connections to the network even with small strength as $\epsilon_2 = 0.01$. It can be seen from Fig. 5a that the complete synchronization cannot be formed in this region, and the pattern of neurons is the asynchronization or the chimera. As the chemical coupling strength increases, the synchrony level increases, although the complete synchronization is not achieved in this region. Fig. 5b represents that with these parameter values and $\epsilon_2 = 0.05$, the pattern is chimera state. When ϵ_2 increases to 0.1, synchronization error decreases more; while for higher ϵ_2 again the synchronization error increases, and asynchronization is observed for particular parameter values (as shown in Fig. 5d for $\epsilon_2 = 0.2$). To find the minimum electrical coupling strength for complete synchronization, the strength of incoherence for $\epsilon_3 = 0.05$ and $\epsilon_2 = 0.01, 0.05, 0.1, 0.2$ are plotted according to electrical coupling strength (Fig. 6). It is observed that increasing the chemical coupling (ϵ_2) until 0.1 causes the chimera region to lessen and enhances synchronization. But a further increase in ϵ_2 to 0.2 disturbs the synchronization considerably.

The exemplary spatiotemporal patterns of the three-weighted network are illustrated in Fig. 7. The panels A-F correspond to the points specified in Fig. 5. Panels A-D, which represent chimera state, refer to lower chemical coupling strengths, i.e., $\epsilon_2 = 0.01$ and $\epsilon_2 = 0.05$. While for $\epsilon_2 = 0.1$, the coherency is increased among neurons, and the pattern is the solitary state, as shown in panel E. In panel F, ϵ_2 raises to 0.2, and the incoherency is raised accordingly. Therefore, the pattern returns to the chimera state. Similar to the two-weighted network, varying the coupling strengths results in the variation of the time series.

In the second step, the network is considered to be directed. Therefore, the effects of the directed links on the chimera state and synchronization can be obtained. Fig. 8 represents the SI and synchrony error of the directed network with two types of couplings in 2D parameter planes. It can be seen that the most remarkable change in the regions happens when $\epsilon_2 = 0$ (part a). As mentioned previously, for $\epsilon_2 = 0$, the synchrony was increased by strengthening ϵ_1 and ϵ_3, although there was an island of chimera region approximately in the interval $\epsilon_1 \in (0.004, 0.0085)$ and $\epsilon_3 \in (0.004, 0.037)$ (Fig. 2a). But this region does not exist in the directed network, and synchronization enhances monotonically by increasing ϵ_1 and ϵ_3.

In the absence of magnetic coupling, the dynamical regions of the undirected and directed networks are almost the same (Fig. 8b). Finally, the dynamical region of the network is slightly changed by using directionally weighted links when the electrical coupling is ignored (Fig. 8c). Comparison of Fig. 2c and Fig. 8c demonstrates that the asynchronous region is enlarged a bit. Furthermore, in the undirected network, the most synchrony was observed around $\epsilon_2 = 0.1$, while in the directed network happens around $\epsilon_2 = 0.12$.

Finally, Fig. 9 depicts the SI and synchrony error for the directed network in the (ϵ_1, ϵ_3) plane, which can be compared with the undirected network in Fig. 5. Fig. 9a shows that the asynchronous region is a bit lessened for $\epsilon_2 = 0.01$; moreover, for $\epsilon_2 = 0.2$, the asynchronization disappears, and the network's behavior is the chimera in all the parameter plane (Fig. 9d). In addition, the value of maximum error is decreased for all ϵ_2 values. Thus, it can

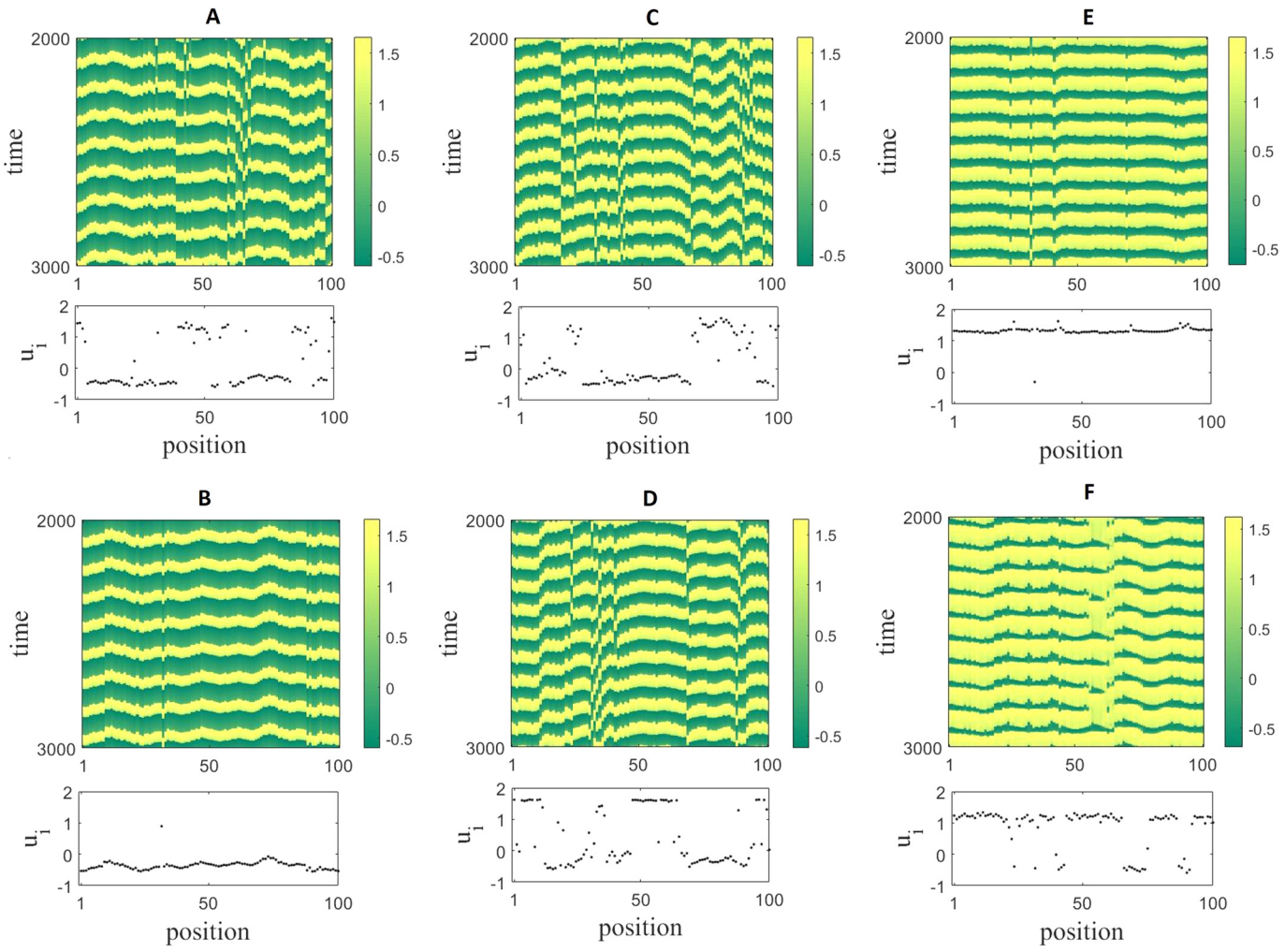

Fig. 7. The evolution of the undirected network with considering three interactions, corresponding to the points specified in Fig. 5. A: $\epsilon_1 = 0.006$, $\epsilon_2 = 0.01$, $\epsilon_3 = 0.008$; B: $\epsilon_1 = 0.008$, $\epsilon_2 = 0.01$, $\epsilon_3 = 0.04$; C: $\epsilon_1 = 0.001$, $\epsilon_2 = 0.05$, $\epsilon_3 = 0.007$; D: $\epsilon_1 = 0.005$, $\epsilon_2 = 0.05$, $\epsilon_3 = 0.02$; E: $\epsilon_1 = 0.002$, $\epsilon_2 = 0.1$, $\epsilon_3 = 0.01$; F: $\epsilon_1 = 0.009$, $\epsilon_2 = 0.2$, $\epsilon_3 = 0.03$. The figure represents the chimera patterns formed by varying the strength of couplings when all types of interactions exist in the network.

be concluded that directed links can enhance synchronization. For more illustration, 1D SI diagrams according to ϵ_1 are represented in Fig. 10 for $\epsilon_3 = 0.05$ and $\epsilon_2 = 0.01, 0.05, 0.1, 0.2$. In contrast to the undirected network, synchronization is achieved for stronger electrical couplings by increasing the chemical coupling strength.

4. Discussion and conclusion

This paper is focused on the synchronization and chimera in a multi-weighted network of memristive Fitzhugh-Nagumo model. It is known that the neurons interact through three types of couplings named electrical synapses, chemical synapses, and ephaptic coupling. In the previous studies, mostly the collective behaviors of the neurons have been investigated with either of these couplings. However, a few have considered hybrid couplings of electrical and chemical synapses in different frameworks. For example, Mishra et al. [50] found the traveling chimera patterns among neurons coupled with local gap junctions and non-local chemical synapses. Hizanidis et al. [49] represented the formation of chimera states in the modular neuronal network with electrical synapses within communities and the electrical synapses between communities. Here, three types of interactions are considered with weighted links constructed by the small-world structure. To quantify the synchronization and the chimera, the synchronization error and the strength of incoherence are computed. At first, the network is considered to be undirected. When considering two types of interactions, the most synchronization level is attained with electrical and magnetic couplings. In contrast, the presence of the chemical and electrical synapses leads to complete synchronization in stronger electrical coupling. This result is consistent with the finding of Refs. [47,48]. In [47], Makarov et al. investigated a multi-scale network of Hindmarsh-Rose neurons. They showed that by increasing the chemical coupling strength, the synchronization is attained by a stronger electrical coupling. However, an inverse result was obtained for strong chemical coupling by changing the connections of the subnetworks. Calim et al. [48] reported a variety of neuronal behaviors for different chemical strengths in weak electrical connections and enhanced synchronization in strong electrical coupling. Moreover, here, we find that by only considering the chemical and magnetic couplings, the synchronization cannot be achieved, and the chimera state is just developed.

Then the three-weighted network is investigated by adding the chemical synapses to the network with electrical and ephaptic couplings. It is observed that the chemical coupling disturbs the synchrony and extends the chimera region. Increasing the chemical coupling strength to a certain value leads to improved synchrony, but a further increase has the opposite effect and increases the threshold of transition from chimera to synchronization. In the

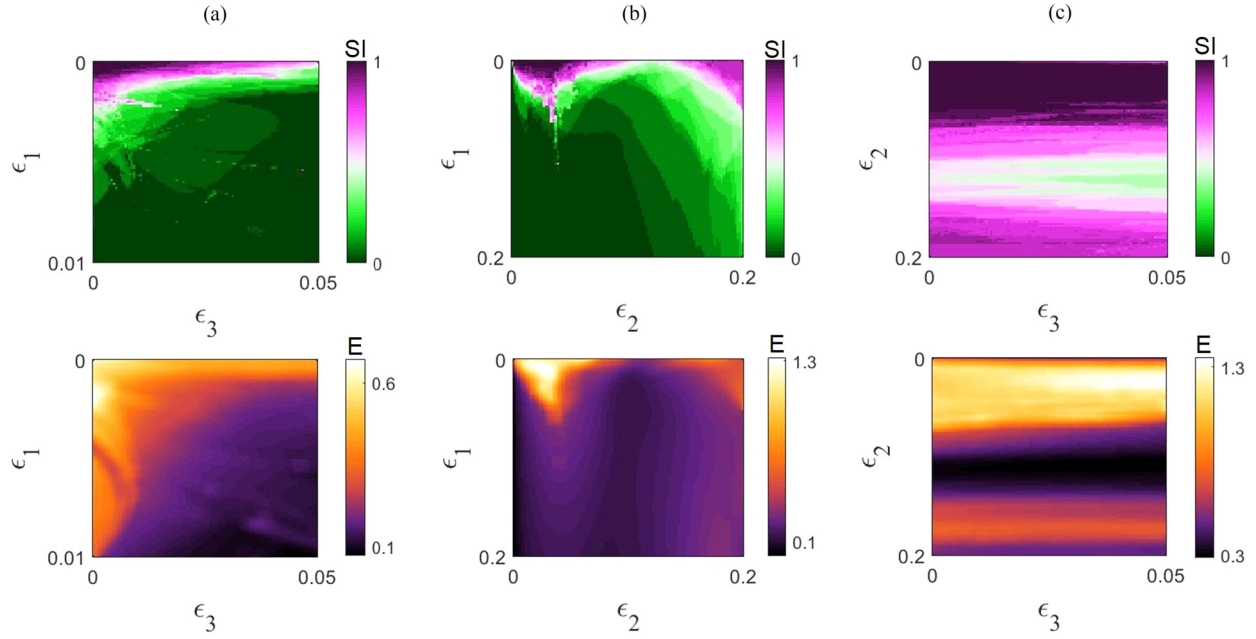

Fig. 8. The strength of incoherence (SI, top row) and the synchronization error (E, bottom row) of the directed multi-weighted network with considering two interactions. (a) In the parameter plane (ϵ_1, ϵ_3), $\epsilon_2 = 0$. (b) In the parameter plane (ϵ_1, ϵ_2), $\epsilon_3 = 0$. (c) In the parameter plane (ϵ_2, ϵ_3), $\epsilon_1 = 0$. Compared with the undirected network (Fig. 2), a part of chimera region in the plane of (ϵ_1, ϵ_3) is removed and changed to synchronization. Furthermore, the asynchronization region in the plane of (ϵ_2, ϵ_3) is extended.

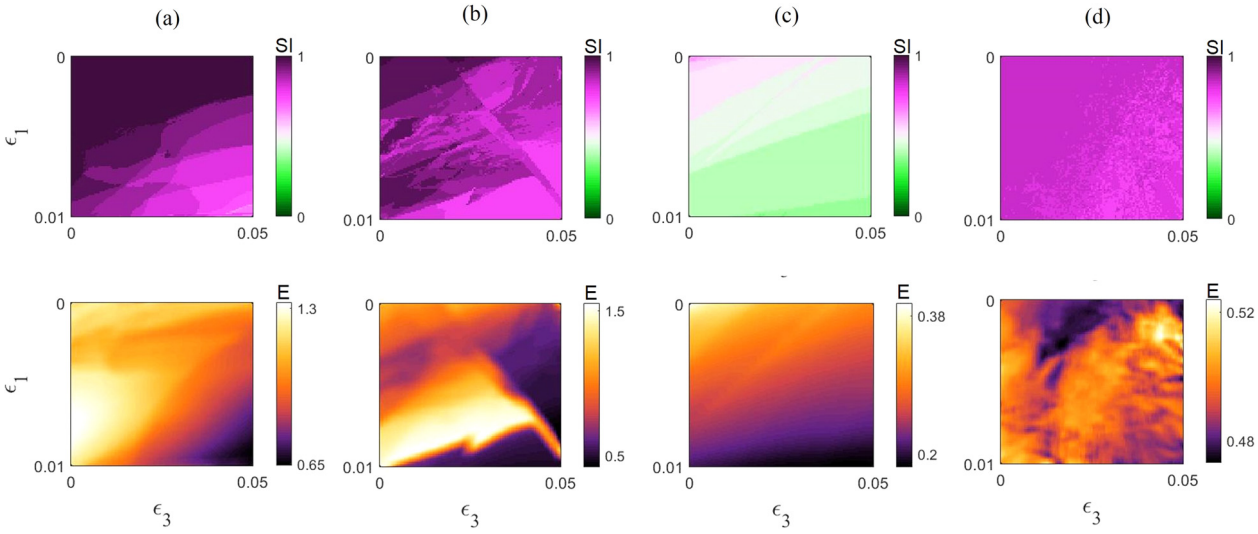

Fig. 9. The strength of incoherence (SI, top row) and the synchronization error (E, bottom row) of the directed multi-weighted network in the parameter plane (ϵ_1, ϵ_3), for different ϵ_2. (a) $\epsilon_2 = 0.01$, (b) $\epsilon_2 = 0.05$, (c) $\epsilon_2 = 0.1$, (d) $\epsilon_2 = 0.2$. Similar to the undirected network, the synchronization is enhanced around $\epsilon_2 = 0.1$. However, the maximum synchronization error is generally lower in the directed network.

next step, the links of the network are assumed to be directed. In the presence of two interactions, the most difference between directed and undirected networks refers to the electrical and magnetic couplings, where the directional links remove a chimera region and extend the synchrony region. However, in the presence of directed chemical and magnetic couplings, the asynchronous region is slightly enlarged. In the three-weighted network, generally, the directed links lead to a decrease in the synchronization error.

CRediT authorship contribution statement

Iqtadar Hussain: Conceptualization, Methodology, Software, Writing – original draft. **Sajad Jafari:** Writing – review & editing, Methodology, Funding acquisition. **Matjaž Perc:** Conceptualization, Methodology, Supervision, Validation, Visualization. **Dibakar Ghosh:** Writing – review & editing, Visualization, Supervision, Funding acquisition, Conceptualization.

Declaration of competing interest

The authors declare that they have no known competing financial interests or personal relationships that could have appeared to influence the work reported in this paper.

Acknowledgements

M.P. was supported by the Slovenian Research Agency (Grant Nos. P1-0403 and J1-2457).

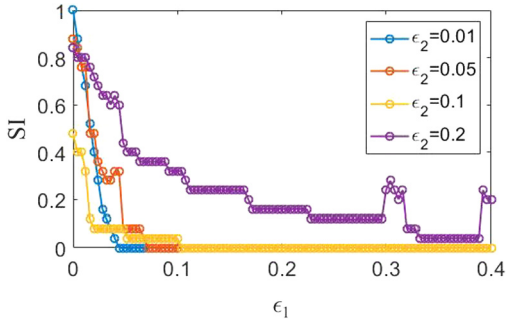

Fig. 10. The strength of incoherence of the directed multi-weighted network according to ϵ_1, for $\epsilon_3 = 0.05$ and $\epsilon_2 = 0.01, 0.05, 0.1, 0.2$. By setting $\epsilon_3 = 0.05$ and increasing the chemical coupling strength, larger electrical coupling is needed for synchronization. This is in contrast to the undirected network (Fig. 6).

References

[1] A. Arenas, A. Díaz-Guilera, J. Kurths, Y. Moreno, C. Zhou, Synchronization in complex networks, Phys. Rep. 469 (3) (2008) 93–153.
[2] S. Boccaletti, A.N. Pisarchik, C.I. Del Genio, A. Amann, Synchronization: from Coupled Systems to Complex Networks, Cambridge University Press, 2018.
[3] I.V. Belykh, V.N. Belykh, M. Hasler, Blinking model and synchronization in small-world networks with a time-varying coupling, Physica D 195 (1–2) (2004) 188–206.
[4] L.M. Pecora, T.L. Carroll, Master stability functions for synchronized coupled systems, Phys. Rev. Lett. 80 (10) (1998) 2109.
[5] M.J. Jutras, E.A. Buffalo, Synchronous neural activity and memory formation, Curr. Opin. Neurobiol. 20 (2) (2010) 150–155.
[6] W. Klimesch, Memory processes, brain oscillations and eeg synchronization, Int. J. Psychophysiol. 24 (1–2) (1996) 61–100.
[7] C. Hammond, H. Bergman, P. Brown, Pathological synchronization in Parkinson's disease: networks, models and treatments, Trends Neurosci. 30 (7) (2007) 357–364.
[8] L. Aron, B.A. Yankner, Neural synchronization in Alzheimer's disease, Nature 540 (2016) 207–208.
[9] S. Rakshit, A. Ray, B.K. Bera, D. Ghosh, Synchronization and firing patterns of coupled Rulkov neuronal map, Nonlinear Dyn. 94 (2) (2018) 785–805.
[10] S. Rakshit, B.K. Bera, D. Ghosh, S. Sinha, Emergence of synchronization and regularity in firing patterns in time-varying neural hypernetworks, Phys. Rev. E 97 (5) (2018) 052304.
[11] M. Ge, Y. Jia, Y. Xu, L. Lu, H. Wang, Y. Zhao, Wave propagation and synchronization induced by chemical autapse in chain Hindmarsh–Rose neural network, Appl. Math. Comput. 352 (2019) 136–145.
[12] S. Rakshit, B.K. Bera, D. Ghosh, Synchronization in a temporal multiplex neuronal hypernetwork, Phys. Rev. E 98 (3) (2018) 032305.
[13] X. Sun, M. Perc, J. Kurths, Effects of partial time delays on phase synchronization in Watts-Strogatz small-world neuronal networks, Chaos 27 (5) (2017) 053113.
[14] S. Majhi, B.K. Bera, D. Ghosh, M. Perc, Chimera states in neuronal networks: a review, Phys. Life Rev. 28 (2019) 100–121.
[15] F. Parastesh, S. Jafari, H. Azarnoush, Z. Shahriari, Z. Wang, S. Boccaletti, M. Perc, Chimeras, Phys. Rep. 898 (2020) 1–114.
[16] D. Nikitin, I. Omelchenko, A. Zakharova, M. Avetyan, A.L. Fradkov, E. Schöll, Complex partial synchronization patterns in networks of delay-coupled neurons, Philos. Trans. R. Soc. Lond., Ser. A 377 (2153) (2019) 20180128.
[17] J. Sawicki, I. Omelchenko, A. Zakharova, E. Schöll, Delay-induced chimeras in neural networks with fractal topology, Eur. Phys. J. B 92 (3) (2019) 1–8.
[18] I. Hussain, S. Jafari, D. Ghosh, M. Perc, Synchronization and chimeras in a network of photosensitive Fitzhugh–Nagumo neurons, Nonlinear Dyn. 104 (2021) 2711–2721.
[19] A.V. Andreev, M.V. Ivanchenko, A.N. Pisarchik, A.E. Hramov, Stimulus classification using chimera-like states in a spiking neural network, Chaos Solitons Fractals 139 (2020) 110061.
[20] J. Ramadoss, S. Aghababaei, F. Parastesh, K. Rajagopal, S. Jafari, I. Hussain, Chimera state in the network of fractional–order Fitzhugh–Nagumo neurons, Complexity 2021 (2021) 2437737.
[21] S. Aghababaei, S. Balaraman, K. Rajagopal, F. Parastesh, S. Panahi, S. Jafari, Effects of autapse on the chimera state in a Hindmarsh-Rose neuronal network, Chaos Solitons Fractals 153 (2021) 111498.
[22] A.V. Andreev, N.S. Frolov, A.N. Pisarchik, A.E. Hramov, Chimera state in complex networks of bistable Hodgkin-Huxley neurons, Phys. Rev. E 100 (2) (2019) 022224.
[23] S. Majhi, M. Perc, D. Ghosh, Chimera states in a multilayer network of coupled and uncoupled neurons, Chaos 27 (7) (2017) 073109.
[24] A. Bahramian, F. Parastesh, V.-T. Pham, T. Kapitaniak, S. Jafari, M. Perc, Collective behavior in a two-layer neuronal network with time-varying chemical connections that are controlled by a Petri net, Chaos 31 (3) (2021) 033138.
[25] T. Chouzouris, I. Omelchenko, A. Zakharova, J. Hlinka, P. Jiruska, E. Schöll, Chimera states in brain networks: empirical neural vs. modular fractal connectivity, Chaos 28 (4) (2018) 045112.
[26] G.R. Simo, P. Louodop, D. Ghosh, T. Njougouo, R. Tchitnga, H.A. Cerdeira, Traveling chimera patterns in a two-dimensional neuronal network, Phys. Lett. A (2021) 127519.
[27] A. Rontogiannis, A. Provata, Chimera states in Fitzhugh–Nagumo networks with reflecting connectivity, Eur. Phys. J. B 94 (5) (2021) 1–12.
[28] G. Ruzzene, I. Omelchenko, J. Sawicki, A. Zakharova, E. Schöll, R.G. Andrzejak, Remote pacemaker control of chimera states in multilayer networks of neurons, Phys. Rev. E 102 (5) (2020) 052216.
[29] P.A. Anderson, Physiology of a bidirectional, excitatory, chemical synapse, J. Neurophysiol. 53 (3) (1985) 821–835.
[30] S. Majhi, M. Perc, D. Ghosh, Chimera states in uncoupled neurons induced by a multilayer structure, Sci. Rep. 6 (1) (2016) 1–11.
[31] A.C. Miller, A.E. Pereda, The electrical synapse: molecular complexities at the gap and beyond, Dev. Neurobiol. 77 (5) (2017) 562–574.
[32] B.K. Bera, S. Majhi, D. Ghosh, M. Perc, Chimera states: effects of different coupling topologies, Europhys. Lett. 118 (1) (2017) 10001.
[33] S. Rakshit, B.K. Bera, E.M. Bollt, D. Ghosh, Intralayer synchronization in evolving multiplex hypernetworks: analytical approach, SIAM J. Appl. Dyn. Syst. 19 (2) (2020) 918–963.
[34] A.E. Pereda, Electrical synapses and their functional interactions with chemical synapses, Nat. Rev. Neurosci. 15 (4) (2014) 250–263.
[35] B.K. Bera, S. Rakshit, D. Ghosh, J. Kurths, Spike chimera states and firing regularities in neuronal hypernetworks, Chaos 29 (5) (2019) 053115.
[36] C.A. Anastassiou, R. Perin, H. Markram, C. Koch, Ephaptic coupling of cortical neurons, Nat. Neurosci. 14 (2) (2011) 217–223.
[37] S. Majhi, D. Ghosh, Alternating chimeras in networks of ephaptically coupled bursting neurons, Chaos 28 (8) (2018) 083113.
[38] M. Lv, C. Wang, G. Ren, J. Ma, X. Song, Model of electrical activity in a neuron under magnetic flow effect, Nonlinear Dyn. 85 (3) (2016) 1479–1490.
[39] M.S. Kafraj, F. Parastesh, S. Jafari, Firing patterns of an improved Izhikevich neuron model under the effect of electromagnetic induction and noise, Chaos Solitons Fractals 137 (2020) 109782.
[40] F. Wu, J. Ma, G. Zhang, A new neuron model under electromagnetic field, Appl. Math. Comput. 347 (2019) 590–599.
[41] G. Ren, Y. Xu, C. Wang, Synchronization behavior of coupled neuron circuits composed of memristors, Nonlinear Dyn. 88 (2) (2017) 893–901.
[42] Y. Xu, Y. Jia, J. Ma, A. Alsaedi, B. Ahmad, Synchronization between neurons coupled by memristor, Chaos Solitons Fractals 104 (2017) 435–442.
[43] M. Ge, L. Lu, Y. Xu, X. Zhan, L. Yang, Y. Jia, Effects of electromagnetic induction on signal propagation and synchronization in multilayer Hindmarsh-Rose neural networks, Eur. Phys. J. Spec. Top. 228 (11) (2019) 2455–2464.
[44] H. Bao, Y. Zhang, W. Liu, B. Bao, Memristor synapse-coupled memristive neuron network: synchronization transition and occurrence of chimera, Nonlinear Dyn. 100 (1) (2020) 937–950.
[45] A. Karthikeyan, I. Moroz, K. Rajagopal, P. Duraisamy, Effect of temperature sensitive ion channels on the single and multilayer network behavior of an excitable media with electromagnetic induction, Chaos Solitons Fractals 150 (2021) 111144.
[46] M. Shafiei, S. Jafari, F. Parastesh, M. Ozer, T. Kapitaniak, M. Perc, Time delayed chemical synapses and synchronization in multilayer neuronal networks with ephaptic inter-layer coupling, Commun. Nonlinear Sci. Numer. Simul. 84 (2020) 105175.
[47] V.V. Makarov, S. Kundu, D.V. Kirsanov, N.S. Frolov, V.A. Maksimenko, et al., Multiscale interaction promotes chimera states in complex networks, Commun. Nonlinear Sci. Numer. Simul. 71 (2019) 118–129.
[48] A. Calim, J.J. Torres, M. Ozer, M. Uzuntarla, Chimera states in hybrid coupled neuron populations, Neural Netw. 126 (2020) 108–117.
[49] J. Hizanidis, N.E. Kouvaris, G. Zamora-López, A. Díaz-Guilera, C.G. Antonopoulos, Chimera-like states in modular neural networks, Sci. Rep. 6 (1) (2016) 1–11.
[50] A. Mishra, S. Saha, D. Ghosh, G.V. Osipov, S.K. Dana, Traveling chimera pattern in a neuronal network under local gap junctional and nonlocal chemical synaptic interactions, OM&P 3 (1) (2017) 14–18.
[51] Y.X. Fu, Y.M. Kang, Y. Xie, Subcritical Hopf bifurcation and stochastic resonance of electrical activities in neuron under electromagnetic induction, Front. Comput. Neurosci. 12 (2018) 6.
[52] B. Xu, S. Binczak, S. Jacquir, O. Pont, H. Yahia, Parameters analysis of Fitzhugh-Nagumo model for a reliable simulation, in: 2014 36th Annual International Conference of the IEEE Engineering in Medicine and Biology Society, IEEE, 2014, pp. 4334–4337.
[53] R. Gopal, V.K. Chandrasekar, A. Venkatesan, M. Lakshmanan, Observation and characterization of chimera states in coupled dynamical systems with nonlocal coupling, Phys. Rev. E 89 (5) (2014) 052914.